Journal of Molecular Catalysis A: Chemical 297 (2009) 44–53

Contents lists available at ScienceDirect

Journal of Molecular Catalysis A: Chemical

journal homepage: www.elsevier.com/locate/molcata

Epoxidation of olefins with H_2O_2 catalyzed by new symmetrical acetylacetone-based Schiff bases/Mn(II) homogeneous systems: A catalytic and EPR study

Ag. Stamatis[a], P. Doutsi[a], Ch. Vartzouma[a], K.C. Christoforidis[b], Y. Deligiannakis[b,*], M. Louloudi[a,*]

[a] Department of Chemistry, University of Ioannina, 45110 Ioannina, Greece
[b] University of Ioannina, Department of Environmental and Natural Resources Management, Laboratory of Physical Chemistry, Pyllinis 9, 30100 Agrinio, Greece

ARTICLE INFO

Article history:
Received 8 July 2008
Received in revised form 3 September 2008
Accepted 5 September 2008
Available online 25 September 2008

Keywords:
Catalytic epoxidation
Manganese complexes
Hydrogen peroxide activation
Additive
EPR

ABSTRACT

Two new symmetrical acetylacetone-based Schiff bases, herein called L_A and L_B, have been synthesized. The complexes formed by their association with Mn(II) have been evaluated for catalytic alkene epoxidation with H_2O_2. The catalytic efficiency of Mn(II)/L_A and Mn(II)/L_B systems were shown to be switched on by ammonium acetate with remarkable effectiveness and selectivity towards epoxides. EPR spectroscopy for Mn(II)/L_A shows that the catalytic centre is a mononuclear Mn complex. Additives that allow easier oxidation of Mn(II) to higher oxidation states, i.e. such as acetate and bicarbonate, can promote decisively the catalytic function. Additives that do not allow oxidation of Mn(II) to higher oxidation states, i.e. such as formate and oxalate, inhibit severely the catalytic function. Monocarboxylate ions, i.e. acetate, bicarbonate and formate do not disturb considerably the first coordination sphere of Mn(II). Dicarboxylate additives, i.e. such as oxalate, form strong complex with the Mn(II).

Based on the catalytic and EPR data, a double role is suggested for ammonium acetate. This is to promote Mn(II) oxidation, and to function as a dual acid-base system, participating into the catalytic cycle.

1. Introduction

Oxidation catalysis constitutes an important research area since it represents the core of a variety of chemical processes for producing bulk and fine chemicals as well as for eliminating pollution. In biology, non-heme manganese-enzymes intervene in a series of oxidation–reduction reactions [1,2]. Among them, activation of H_2O_2 by non-heme manganese-enzymes is well known [1,2]. Concomitantly, the challenge in the field of biomimetic chemistry is to construct low-molecular weight metal complexes aiming to reproduce structural and functional features of pertinent enzymes.

In the last years olefin epoxidations with hydrogen peroxide catalyzed by non-heme manganese complexes has received considerable attention mainly for two reasons: (a) non-heme manganese complexes are often easily prepared, handled and accessible as catalysts [3], and (b) hydrogen peroxide is the most attractive primary oxidant since it is inexpensive, readily available with relatively high oxygen content and environmentally friendly, leaving only water as waste product [3].

Mn-salen-type complexes have been extensively studied as epoxidation catalysts, with special attention to asymmetric catalysis [4]. In 1990, the groups of Jacobsen and Katsuki independently introduced a chiral diamine group in the salen-ligand [5,6]. Bulky substituents at near axial coordination sites have been shown to prohibit formation of octahedral inactive manganese complexes and, at the same time, enhance the performance of the Mn-salen catalysts [5,6]. At that time the use of H_2O_2 as oxidant was limited [7] since the most commonly used oxidants were iodosylbenzene and sodium hypochlorite. Moreover, it was proposed that the main problem in Mn-salen catalyzed epoxidations by H_2O_2 was the formation of $HO^{\bullet}$ radicals by the homolytic cleavage of the O—O bond, leading to the indiscriminate oxidation [8]. Addition of Lewis bases, such as imidazole, pyridine, or 2,6-lutidine, was found to favor heterolytic bond cleavage, leading to reactive manganese-oxo species [9,10]. Adducts like $Ph_3P(O)\cdot H_2O_2$ with maleic anhydride and urea·H_2O_2 with ammonium acetate have been used alternatively [11].

In 1993, Berkessel reported asymmetric epoxidation of unfuctionilized 1,2-dihydronaphthalene with H_2O_2, catalyzed by a manganese complex of a chiral pentadentate dihydrosalen ligand bearing a covalently attached imidazole [12]. For the epoxidation of simple olefins, the Jacobsen-type catalysts and *in situ* addition of imidazole or N-methylimidazole have been used also [7,13].

* Corresponding authors.
E-mail addresses: ideligia@cc.uoi.gr (Y. Deligiannakis), mlouloud@uoi.gr (M. Louloudi).

1381-1169/$ – see front matter © 2008 Elsevier B.V. All rights reserved.
doi:10.1016/j.molcata.2008.09.019

The group of Reedijk has investigated the catalytic performance of manganese complexes with 2-(2′hydroxyphenyl)oxazoline. Their relatively low catalytic activity has been attributed to the saturated hexa-coordinated metal center which prevents substrate access [14,15].

The use of Mn–Me_3TACN complexes, as promising oxidation catalysts has been explored by the work at Unilever for washing detergents [16]. This system was further improved by the work of De Vos and Bein [17] where it has been shown that peroxide disproportionation is suppressed in acetone favouring alkene epoxidation [17]. In addition, it was reported that the $[Mn(Me_3TACN)(OMe)_3](PF_6)$ complex was able to activate H_2O_2 in water and to effectively oxidize catalytically water-soluble olefins [18]. The addition of co-catalysts such as oxalate/oxalic acid [19], ascorbic acid [20], glyoxylic acid methylester methyl hemiacetal [21] or simple carboxylic acid [22] has further improved the catalytic effectiveness of Mn–Me_3TACN systems. Very recently, it was shown that the high activity and selectivity of these systems is due to the *in situ* formation of bis(μ-carboxylato)-bridged dinuclear manganese(III) complexes [23,24].

A very simple catalytic system of $MnSO_4$ in a carbonate buffer has been reported [25,26]. The mixture of hydrogen peroxide and hydrogen carbonate produces a peroxycarbonate *via* an equilibrium which is established in a few minutes. However, the epoxidation reactions required 24 h to be accomplished. In 2000, Feringa and co-workers [27] have synthesized an efficient dinuclear manganese catalyst based on polypyridine ligands introducing a three nitrogen donor set for each manganese center [27].

However, new, efficient, selective, low-cost and easy-to-prepare manganese catalysts remain at high demand in the field of hydrocarbon oxidation by H_2O_2. Within this context, during the last years, our group, has developed imidazole based-acetamide/Mn(II) systems [28,29] and acetylacetone-based Schiff bases/Mn(II) systems [30,31] as homogeneous catalysts for alkene epoxidation with H_2O_2. These systems showed considerable effectiveness in an acetone–methanol mixture at room temperature in the presence of ammonium acetate as additive. Here, we continue our contribution in this field by presenting new symmetrical acetylacetone-based Schiff base/Mn(II) systems and their evaluation as homogeneous catalysts for alkene epoxidation with H_2O_2. These systems are ammonium acetate-dependent also and they show remarkable effectiveness and selectivity. The role of ammonium acetate into the catalytic reactions has been investigated and implications concerning its function are also discussed.

2. Experimental

All substrates were purchased from Aldrich, in their highest commercial purity, stored at 5 °C and purified by passage through a column of basic alumina prior to use. Hydrogen peroxide was 30% aqueous solution.

Elemental analyses (C, H, N) were obtained using a PerkinElmer Series II 2400 elemental analyzer. Infrared spectra were recorded on a Spectrum GX PerkinElmer FT-IR System and UV–Vis spectra were recorded using a UV/VIS/NIR JASCO Spectrophotometer. Continuous-wave (c.w.) Electron Paramagnetic Resonance (EPR) spectra were recorded with a Brucker ER200D spectrometer at liquid N_2 temperatures, equipped with an Agilent 5310A frequency counter. The spectrometer was running under a home-made software based on LabView. Mass spectra were measured on a Agilent 1100 Series LC-MSD-Trap-SL spectrometer and solution NMR spectra were recorded with a Bruker AMX-400 MHz spectrometer with external TMS as reference. Thermogravimetric analyses were carried out using Shimadzu DTG-60 analyser. GC analysis was performed using a 8000 Fisons chromatograph with a flame ionization detector and a Shimadzu GC-17A gas chromatograph coupled with a GCMS-QP5000 mass spectrometer. Solution potential E_h was measured by a Metrohm platinum redox electrode (type 6.0401.100).

2.1. Catalytic reactions

A 0.055 M stock solution of the catalysts was prepared by dissolving 1.1 mmol of L_A or L_B in a 0.110 M solution of $MnCl_2{\cdot}4H_2O$ or $Mn(CH_3COO)_2{\cdot}4H_2O$ in 20 ml CH_3OH. The alkene (1 mmol), acetophenone or bromobenzene (internal standard, 1 mmol), catalyst solution (1 μmol) and additive (typically 1 mmol of CH_3COONH_4) in a acetone/MeOH (450 μl/400 μl) solvent mixture were cooled to 0 °C. H_2O_2 (2 mmol) was added by a digitally controlled syringe pump type SP101IZ WPI over 1 h under stirring. 10 min later, the test tube was removed from the ice bath and allowed to warm to room temperature 26 ± 1 °C. The progress of the reaction was monitored by GC–MS, by removing small samples of the reaction mixture. GC analysis of the solution provided the substrate conversion and product yield relative to the internal standard integration. To establish the identity of the epoxide product unequivocally, the retention time and spectral data were compared to those of an authentic sample. Blank experiments showed that without Mn-catalyst or CH_3COONH_4, epoxidation reactions do not take place.

2.2. EPR experiments

All EPR measurements were conducted in quartz EPR tubes of 3 mm. 80 μl of a stock solution of 5.5 mM Mn(II)/L_A in acetone/MeOH 1/1 (v/v) were added in EPR tubes followed by the addition of 20 μl of aqueous stock solution of 550 mM additive so that the final ratio Mn-L_A/additive was 1/20. Due to solubility problems in the case of $(COONH_4){\cdot}H_2O$ a stock solution of 225 mM was used leading to a ratio Mn-L_A/additive of 1/10. To study the oxidation effect, the redox potential of the stock solution was adjusted at 350 mV by 20 μl of H_2O_2 followed by the addition of the additives.

3. Results and discussion

3.1. Synthesis of the ligands

The Schiff bases L_A and L_B were prepared by a stepwise condensation of trien with two equivalents of acetylacetone or 1,1,1-trifluoro-pentan-2,4-dione, respectively, and 4-hydroxybenzaldehyde in a 1:2:1 molar ratio (Scheme 1).

The five-member imidazolidine ring was formed at the ethylenediamine backbone with 4-hydroxybenzaldehyde according to D. Ray [32]. Thus, two symmetrical N_4O_3 Schiff bases were synthesized via *in situ* imidazolidine ring formation with a pendent 4-hydroxybenzyl-group (synthetic details in Supporting Information). The presented ligands L_A and L_B were the only isolated products. At mass spectra, the molecular peaks for $[MH]^+$ and $[M+Na]^+$ exhibit at *m*/*z* 415, 437 and 523, 545, respectively (see Figs. S1 and S2 in Supporting Information). The IR bands at 1607 and 1612 cm^{-1} were attributed to the imine-stretching bands, ν(C=N). ^1H and ^{13}C NMR spectral assignments for the L_A and L_B were consistent with the proposed formulations (see Supporting Information). For example, in the ^{13}C NMR spectrum of L_A, the signals at 163.4 and 193.6 ppm were attributed to the imine- and keto-carbon atoms, respectively. For L_B, the imine-carbon resonance was detected as a singlet at 170.7 ppm, while the keto-carbon was appeared at 172.8 ppm as a quarter attributing to its connection with the trifluoro-methyl substituents (q, $^2J_{C-F}$ = 30.6 Hz, O=C–CF_3). In the ^1H NMR spectra of L_A and L_B the phenolic OH resonance was located

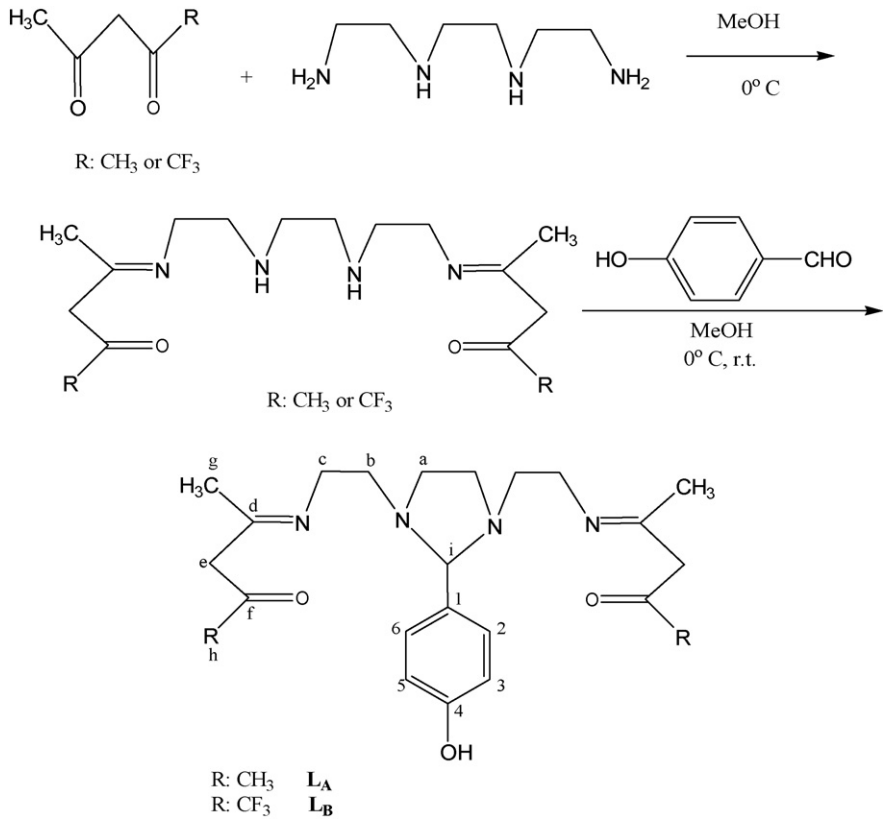

Scheme 1. Synthesis of the ligands.

at 10.5 and 10.8 ppm, respectively. In accordance with literature data, no enolic OH signal was observed confirming the diketone form of both ligands in solution [28]. It is of interest to notice that in the solid state the enolic tautomer prevails, whilst in solution the keto-form is adopted.

3.2. Catalytic epoxidation with H_2O_2

Manganese complexes were prepared *in situ* by mixing appropriate amounts of $MnCl_2$ or $Mn(CH_3COO)_2$ with ligands L_A and L_B. Then the complexes were evaluated as epoxidation catalysts using H_2O_2 as oxidant. Typical reaction conditions employed in these reactions were 1 equiv. of catalyst, 2000 equiv. of H_2O_2 30% delivered by the syringe pump during 1 h into an [acetone:methanol] (0.45 ml:0.40 ml) solution, 1000 equiv. of substrate and ammonium acetate (1000 equiv.) at 0 °C. After 10 min, the reaction mixture was removed from the ice bath and allowed to warm to room temperature. $MnCl_2/L_A$, $MnCl_2/L_B$, $Mn(acet)_2/L_A$ and $Mn(acet)_2/L_B$ systems showed significant catalytic activity within 3 h (Table 1) in comparison to $MnCl_2$ and $Mn(CH_3COO)_2$ which are poor catalysts under the same experimental conditions. However the manganese salts exhibit some catalytic performance within 24 h (Table 1, see Figs. 1 and 2).

According to the data in Table 1, epoxidation of a wide range of olefins proceeds with high conversion and selectivity for the epoxide product (the mass balance is 98–100%) in most of the cases (Table 1). For example, the oxidation of cyclooctene provides a 100% selectivity for *cis*-cyclooctene epoxide with 71.8% and 64.6% yield and 100% m.b. catalysed by $MnCl_2/L_A$ and $MnCl_2/L_B$, respectively (see Fig. 3). When the $Mn(acet)_2/L_A$ and $Mn(acet)_2/L_B$ catalytic systems used, the *cis*-epoxide was also the only product and the obtained yields were 57.4% and 71.3% (see Figs. S3, S4 and S5 in Supporting Information).

Hexene-1 is a rather hard oxidation substrate showing epoxide yields from 14.7% to 18.6% and selectivity 100% for the *cis*-epoxide. Cyclohexene achieves moderate epoxide yields, ranging from 43.2% to 49.9%. In addition, small amounts of the corresponding diol, probably as epoxide ring opening product, have been also detected (1.4–3.3%). In some extent, allylic oxidation has also occurred with the formation of 2-cyclohexene-1-ol and 2-cyclohexene-1-one. The alcohol derivative determined to be 2.5–3.2% and the yield of the corresponding ketone is 3.4–4.4%. Overall, cyclohexene is epoxidized by the present catalytic systems with 83–88% selectivity

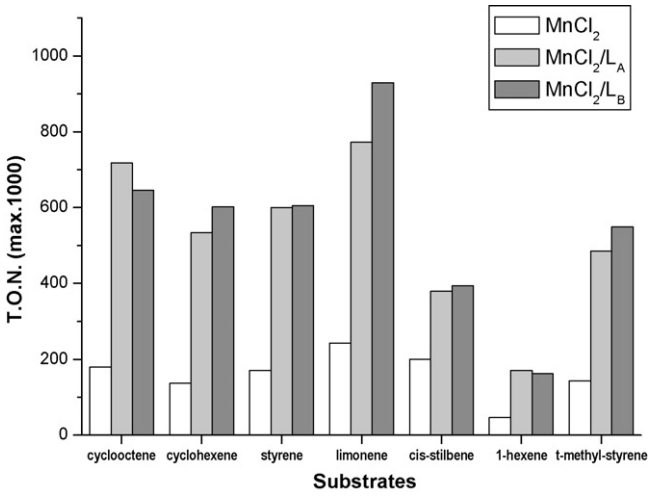

Fig. 1. Bar chart representation of alkene epoxidations catalyzed by $MnCl_2$, $MnCl_2/L_A$ and $MnCl_2/L_B$ in the presence of H_2O_2. Reaction performed in CH_3COCH_3/CH_3OH (0.45:0.40 ml). See Table 1 for details.

Table 1
Alkene epoxidations catalyzed by manganese systems in the presence of H_2O_2[a].

Substrate	Products	$MnCl_2$[e]			$MnCl_2/L_A$[f]			$MnCl_2/L_B$[f]			$Mn(acet)_2$[e]			$Mn(acet)_2/L_A$[f]			$Mn(acet)_2/L_B$[f]		
		Yield (%)[b]	TON[c]	TOF[d] (h^{-1})	Yield (%)[b]	TON[c]	TOF[d] (h^{-1})	Yield (%)[b]	TON[c]	TOF[d] (h^{-1})	Yield (%)[b]	TON[c]	TOF[d] (h^{-1})	Yield (%)[b]	TON[c]	TOF[d] (h^{-1})	Yield (%)[b]	TON[c]	TOF[d] (h^{-1})
Cyclooctene	*cis*-Epoxide	18.0	180	8	71.8	718	239	64.6	646	215	16.8	168	7	57.4	574	191	71.3	713	238
Hexene-1	*cis*-Epoxide	4.6	46	2	17.0	170	57	16.2	162	54	4.1	41	2	14.7	147	49	18.6	186	62
Cyclohexene	*cis*-Epoxide	13.1			45.8			49.9			12.4			43.2			49.4		
	2-Cyclohexenone	0.4	137	6	3.4	534	178	4.3	602	201	0.4	131	5	3.8	518	173	4.4	603	201
	2-Cyclohexenol	0.2			2.8			3.2			0.2			2.5			3.2		
	cis-Diol	–			1.4			2.8			0.1			2.3			3.3		
Styrene	*cis*-Epoxide	17.1	171	7	59.2	600	200	59.3	605	202	12.4	124	5	42.4	433	144	51.5	525	175
	Phenyl acetaldehyde	–			0.8			1.2			–			0.9			1.0		
trans-Methyl-styrene	*trans*-Epoxide	14.3	143	6	48.5	485	162	53.9	549	183	14.9	149	6	51.2	524	175	47.5	485	162
	trans-Methylketone	–			–			1.0			–			1.2					
Limonene[g]	1,2-Epoxides	21.0			61.4			73.7			20.4			58.2			61.8		
	(*cis*-/*trans*-)	(11.8/9.2)			(34.1/27.3)			(41.3/32.4)			(11.7/8.7)			(32.5/25.7)			(33.3/28.5)		
	8,9-Epoxides	3.3	243	10	11.2	772	257	13.8	929	331	3.2	237	10	11.5	740	247	12.8	803	268
	-Alcohol	0.1			2.4			2.6			0.1			2.1			2.7		
	-Ketone				1.1			1.4						1.3			1.5		
	Di-epoxide				1.1			1.4						0.9			1.5		
cis-Stilbene	*cis*-Epoxide	17.1			29.4			30.7			16.6			28.0			33.3		
	trans-Epoxide	2.6	200	8	4.6	379	126	4.7	394	131	2.6	194	8	4.3	361	120	5.2	438	146
	-Ketone	0.3			3.9			4.0			0.2			3.8			5.3		

[a] Conditions-ratio of catalyst:H_2O_2:CH_3COONH_4:substrate= 1:2000:1000:1000; equivalent of catalyst = 1 μmol in 0.85 ml CH_3COCH_3:CH_3OH (0.45:0.40).
[b] Yields based on starting substrate and products formed. The mass balance is 98–100%.
[c] TON: total turnover number, moles of products formed per mole of catalyst.
[d] TOF: turnover frequency which is calculated by the expression [epoxide]/[catalyst] × time (h^{-1}).
[e] Reactions were completed within 24 h.
[f] Reactions were completed within 3 h.
[g] Limonene 1,2-oxide was found as a mixture of *cis*- and *trans*- isomers and limonene 8,9-oxide as a mixture of two diastereoisomers.

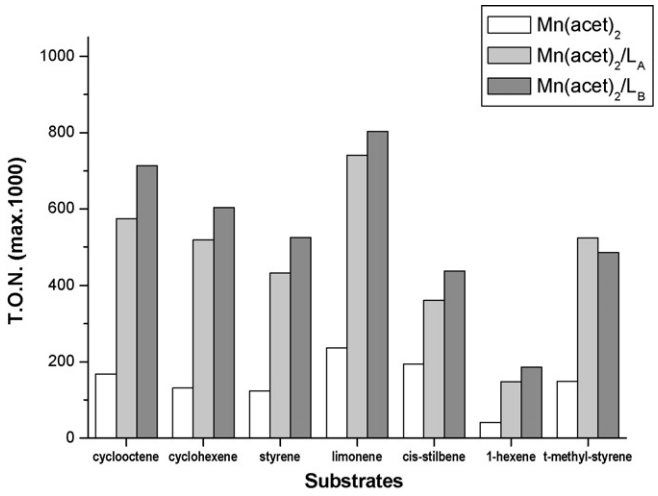

Fig. 2. Bar chart representation of alkene epoxidations catalyzed by $Mn(acet)_2$, $Mn(acet)_2/L_A$ and $Mn(acet)_2/L_B$ in the presence of H_2O_2. Reaction performed in CH_3COCH_3/CH_3OH (0.45:0.40 ml). See Table 1 for details.

(See Figs. 3, S3, S4 and S5). Styrene oxidation produces mainly *cis*-epoxide with yields from 42.4% to 59.2%, and high selectivities up to 99%; trace amounts of phenyl acetaldehyde as side product have been detected. The catalysts showed analogous ability towards the oxidation of *trans*-methylstyrene resulted in 47.5–53.9% epoxide yield with >99% retention of its configuration. Traces of the corresponding methyl-ketone have been also observed (1.0–1.2%). The major products detected from oxidation of limonene, were two epoxides (*cis*- and *trans*-) derived from epoxidation of the electron-rich double bond in 1,2-position and two diastereoisomers derived from the more accessible but less electron-rich double bond in 8,9-position. Additionally, small amounts of products formed by allylic oxidation of the limonene ring have been observed. These were identified as the corresponding derivatives of cyclohexene-1-ol and cyclohexene-1-one. The total yield of epoxides (1,2- plus 8,9-) was varied from 69.7% to 87.5%. It is noted that an additional 1.0–1.5% of di-epoxide has been also formed. The corresponding cyclohexene-1-ol was detected from 2.1% to 2.7% and the corresponding cyclohexene-1-one from 1.1% to 1.5%. However, the

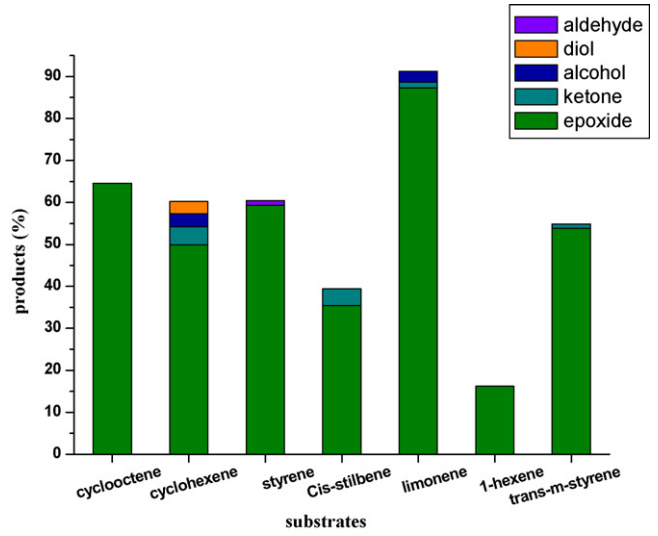

Fig. 3. Distribution of oxidation products catalyzed by $MnCl_2/L_B$ in the presence of H_2O_2. Reaction performed in CH_3COCH_3/CH_3OH (0.45:0.40 ml). See Table 1 for further details.

Table 2
Chemo- and region-selectivity in alkene epoxidation with H_2O_2 catalysed by $MnCl_2/L_A$ and $MnCl_2/L_B$[a].

Alkene 1	Alkene 2	Epoxide 1/epoxide 2[b]	
		$MnCl_2/L_A$	$MnCl_2/L_B$
Styrene	*trans*-Methylstyrene	0.86	0.80
Styrene	*cis*-Stilbene	0.99	0.73
Cyclooctene	Styrene	2.44	2.37
Cyclooctene	Cyclohexene	1.02	1.08
Cyclohexene	Hex-1-ene	12.46	11.78
Cyclohexene	1-Methylcyclohexene	0.75	0.85
Limonene[c]		5.48	5.34

[a] Conditions-ratio of catalyst:H_2O_2:CH_3COONH_4:substrate= 1:2000:1000:1000; equivalent of catalyst = 1 μmol in 0.85 ml CH_3COCH_3:CH_3OH (0.45:0.40). Reactions were usually complete within 3 h.
[b] Yields based on starting substrate.
[c] 1,2- *vs*. 8,9-epoxides.

epoxidation was clearly the main reaction path resulting mainly in 1,2-epoxides (see Table 2, Figs. 3, S3, S4 and S5). The ratio of the 1,2- and 8,9-epoxides was found to be close to 5.4 for both $MnCl_2/L_A$ and $MnCl_2/L_B$ systems and it was calculated at 5.1 and 4.8 for the $Mn(acet)_2/L_A$ and $Mn(acet)_2/L_B$ systems, respectively. In the oxidation of *cis*-stilbene, the major product was *cis*-epoxide with selectivity of 76–78% and yield ranging from 28.0% to 33.3%. Moreover, considerable amounts of trans-stilbene epoxide (4.3–5.2%) and 1,2-diphenyl ethanone (3.8–5.3) have been also detected.

Competitive reactions show alkene reactivity to increase with the electron density of the double bond, e.g. hex-1-ene < cyclohexene < 1-methylcyclohexene (Table 2). These data might be taken as evidence of the electrophilic nature of oxygen transfer from manganese-oxo intermediate to the olefinic double bond. However, additional effects of alkene shape are obvious. For example, the electron-rich trisubstituted double bond of limonene in 1,2-position gives several times more epoxides than the more accessible but less electron-rich double bond in 8,9-position. The reactivity of other substrate types was briefly investigated and the results are listed in Table 2.

3.3. Solvent dependence on the reactivity of $MnCl_2/L_A$

The influence of solvents in the epoxidation of cyclooctene catalysed by $MnCl_2/L_A$ was explored. It was found that the highest conversion of substrate was achieved in a methanol–acetone mixture. The [methanol:acetone] ratio was found to have decisive influence on the reactivity of the catalytic system. The optimum corresponds to [methanol:acetone] [400/450, v/v] (see Fig. 4). Attempts to decrease the amounts of MeOH–acetone by CH_2Cl_2 had a deleterious effect on the epoxidation yield. When a triadic MeOH–acetone–CH_3CN system was tested, the reaction yield was non-zero, however, the yields observed were far lower than those obtained into a MeOH–acetone (400/450, v/v) mixture (see Fig. 5).

3.4. Dependence of catalysts' reactivity on solution redox potential, E_h

According to our data the catalytic reactions were practically accomplished within 3 h. The time course profiles of the $MnCl_2/L_A$- and $MnCl_2/L_B$-catalysed epoxidations of cyclooctene in conjunction with the observed redox potential of solution E_h (*vs*. standard hydrogen electrode SHE) are given in Figs. 6 and 7. At the beginning of the reaction catalysed by $MnCl_2/L_A$ E_h was found to be +363 mV; after 1 h, it dropped at +260 mV with a 50% epoxide yield and finally, after a reaction time of 5 h, it approached a value of E_h = +230 mV with a 70% yield. In the case of $MnCl_2/L_B$-catalysed

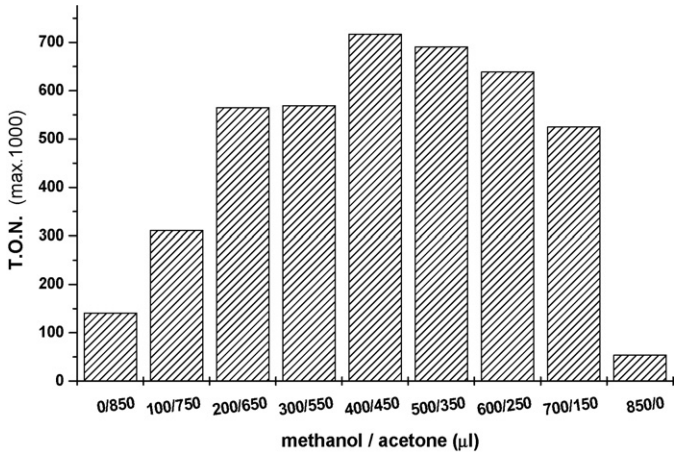

Fig. 4. Total turnover number for cyclooctene epoxidation catalyzed by $MnCl_2/L_A$ at different methanol–acetone solvent mixture. In any case, the total volume of the solvents was fixed and equal to 0.850 ml.

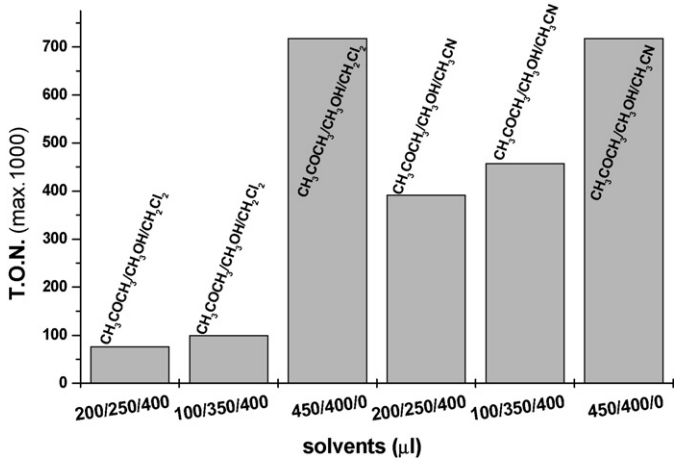

Fig. 5. Solvent dependence of the epoxidation of cyclooctene catalyzed by $MnCl_2/L_A$.

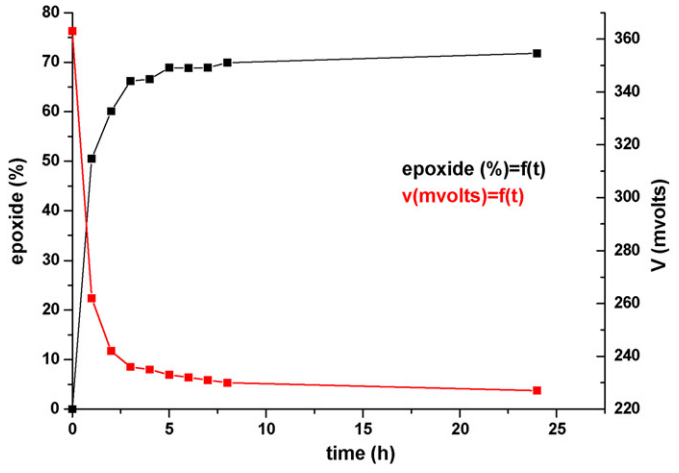

Fig. 6. Time dependence of cyclooctene epoxidation [black line] and solution redox potential [red line] for the same reaction catalysed by $MnCl_2/L_A$. (For interpretation of the references to color in this figure legend, the reader is referred to the web version of the article.)

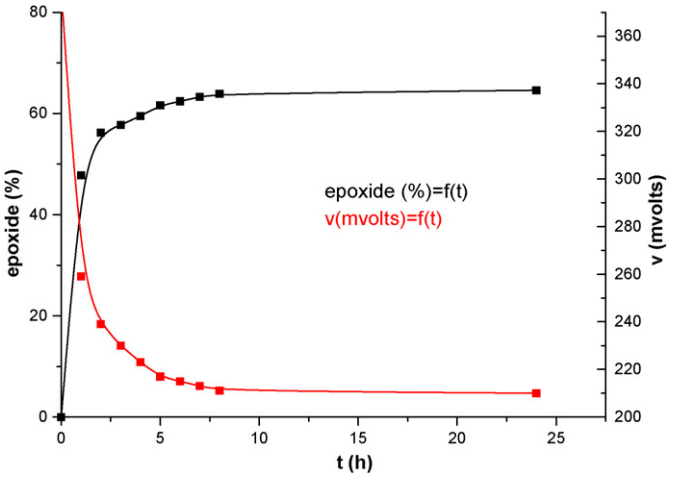

Fig. 7. Time dependence of cyclooctene epoxidation [black line] and solution redox potential [red line] for the same reaction catalysed by $MnCl_2/L_B$. (For interpretation of the references to color in this figure legend, the reader is referred to the web version of the article.)

epoxidation, at reaction time $t = 0$, E_h was found to be +379 mV, at $t = 1$ h, it decreased at +259 mV providing a product yield of 48% and at $t = 5$ h, the E_h approached the +217 mV with a 62% cyclooctene epoxide formation. Additions of new amounts of oxidant were not able to increase the E_h. Subsequent epoxidation of the remaining substrate did not occur.

3.5. Dependence of catalysts' reactivity on additives

A stricking finding of the present experiment was that the catalytic systems needed CH_3COONH_4 as additive for a maximum efficiency. The effect of the added amounts of CH_3COONH_4 on the cyclooctene oxidation catalysed by $MnCl_2/L_A$ has been studied in more detail. The results are presented in Fig. 8. The higher product yield was obtained for a ratio [substrate:CH_3COONH_4] ~ [1:1]. A variety of compounds has been tested as additives for the same catalytic reaction and the observed yields in 24 h, which are actually almost similar with those observed in 3 h, are shown in Table 3. Accordingly we notice that the addition of CH_3COONa, NH_4Cl, imi-

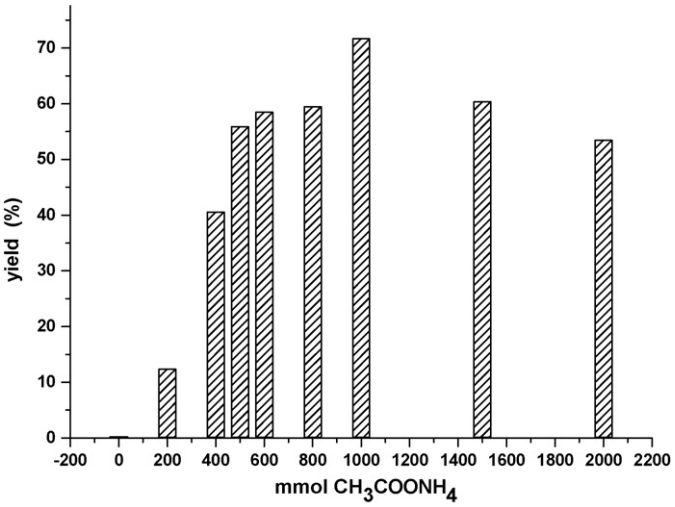

Fig. 8. Effect of relative CH_3COONH_4 concentration on the catalytic epoxidation of cyclooctene by $MnCl_2/L_A$ in the presence of H_2O_2. Reaction performed in CH_3COCH_3/CH_3OH (0.45:0.40 ml).

Table 3
Epoxidation of cyclooctene with H_2O_2 catalyzed by $MnCl_2/L_A$ in the presence of various additives[a].

Additive	Yield (%)[b]
CH_3COONH_4	71.8
Imidazole	–
Pyridine	3.5
Oxalate acid	1.1
HCOOH	2.4
NH_4Cl	–
CH_3COONa	–
Acetylacetone	–
$NaHCO_3$	8.6
$Na_2CO_3{\cdot}10H_2O$	–
$(COONH_4)_2{\cdot}H_2O$	1.7
HCOONH4	5.3
NH_4HCO_3	38.0
$(NH_4)_2SO_4$	–

[a] Conditions-ratio of catalyst:H_2O_2:additive:substrate= 1:2000:1000:1000; equivalent of catalyst = 1 μmol in 0.85 ml CH_3COCH_3:CH_3OH (0.45:0.4).
[b] Yields based on starting substrate after 24 h.

dazole, HCOOH, oxalate acid, $(COONH_4)_2$ and $(NH_4)_2SO_4$ provides very low, i.e. 0–3.5% epoxidation yields. The use of $HCOONH_4$ results in a poor yield of 5.3% and the use of $NaHCO_3$ in 8.6%. Finally when NH_4HCO_3 was added, a relatively high yield 38.0% was obtained which, however, is much lower from the yield of 71.8% obtained with CH_3COONH_4 as additive (Table 3). Investigating the possibility ammonium acetate to act as a coordinative agent, manganese acetate was also used as manganese source. However the data showed that for efficient epoxidations catalysed by $Mn(acet)_2/L_A$ and $Mn(acet)_2/L_B$, ammonium acetate is also required. Moreover, cyclooctene oxidation catalysed by $Mn(acet)_2/L_A$ in the presence of the abovementioned additives was also explored and it presents the same catalytic tendency as the $MnCl_2/L_A$ system.

Overall these data imply that CH_3COONH_4 or, at least, NH_4HCO_3 is required for efficient catalytic performance. In an effort to better understand the physicochemical details, we have performed EPR spectroscopic experiments.

3.6. EPR spectroscopy of $MnCl_2/L_A$ with additives under reaction conditions

3.6.1. Single additive

Fig. 9 shows low temperature EPR spectra of $MnCl_2/L_A$ interacting with the five additives used in the catalytic experiments. The EPR spectrum of $MnCl_2/L_A$ in 1:1 acetone:MeOH (spectrum (a)) is typical for mononulcear Mn(II) ($S = 5/2$, $I = 5/2$) centres with well resolved allowed ^{55}Mn ($S = 5/2$, $I = 5/2$) hyperfine splittings in the range 94–108 Gauss, e.g. due to the well understood m_I dependence of the splittings [33]. Control experiments for $MnCl_2$, i.e. with no L_A present, in 1:1 acetone:MeOH demonstrate that the EPR spectrum in Fig. 9(a) is due to the presence of L_A. The difference lies mainly in the intensity and position of the semiforbidden EPR lines, marked by the downward-pointing arrows, in Fig. 9. Importantly, the analysis of the EPR spectrum based on the splittings of the semiforbidden EPR transitions, marked as 'ΔB' in Fig. 9, using the method of Misra [34] or the intensity method of Allen [35] shows that that the Zero-Field Splitting (ZFS) parameter D is small 0.35 ± 0.05 GHz. This low D-value provides evidence for a weak ligand field imposed by the ligand L_A upon coordination to Mn(II).

Upon addition of 20 μl H_2O the EPR spectrum for $MnCl_2/L_A$ in 1:1 acetone:MeOH shows small-though resolvable-changes (spectrum (9b)). Analysis of the EPR spectrum reveals a rather small change of D parameter, e.g. $D = 0.38 \pm 0.05$ GHz. The small though resolvable change of the ZFS parameter, is indicative of a specific effect, for example coordination of H_2O or OH to Mn(II).

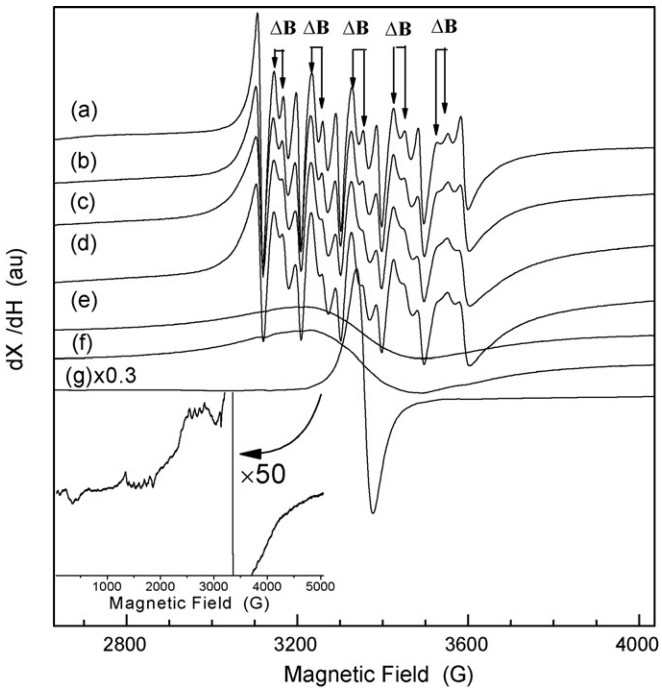

Fig. 9. Effect of co-catalysts on the EPR spectrum of $MnCl_2/L_A$ in (a) acetone/MeOH 1/1 (v/v), with addition of (b) 20 μl H_2O, (c) CH_3COONH_4, (d) $HCOONH_4$, (e) NH_4HCO_3, (f) $NaHCO_3$, (g) $(COONH_4)_2{\cdot}H_2O$. Inset plot zoom of spectrum (g). Experimental conditions: temperature 77 K, modulation amplitude 5 G, microwave power 10 dB.

By addition of either acetate, i.e. CH_3COONH_4 or formate, i.e. $HCOONH_4$ (spectra (c) and (d), respectively), the EPR spectral shape – therefore the D parameter – show a resolvable, though small change *vs*. spectra (a) or (b). This shows that the added molecules coordinate on the Mn(II) center. The D parameter 0.45 ± 0.01 GHz, for acetate, and 0.48 ± 0.01 GHz for formate, shows that they induce a change in the Zero Filed Splitting of the Mn(II) center, however the D values remain small, i.e. typical for mononuclear weakly coordinated Mn(II) complexes [33]. In addition, the hyperfine features are broader, resulting in an apparent intensity decrease by ~20% relative to spectrum (a). Careful integration of the EPR spectra recorded under non-saturating condition shows that in all cases integrated EPR spectra have the same area. This indicates that the intensity changes observed in the first-derivative EPR spectra, in Fig. 9, are not due to redox events, i.e. for example Mn(II) oxidation, but rather due to lineshape broadening.

In the case of bicarbonate salts, i.e. NH_4HCO_3 or $NaHCO_3$ (spectra (e) and (f)), the EPR spectra were broad featureless derivatives with only faintly resolved hyperfine structure. Integration of the EPR spectra show that the broadening does not change the number of Mn(II) spins. Thus, as in the case of the other additives, redox events do not occur in the presence of bicarbonate salts. The observed broadening most likely is due to weak magnetic couplings between neighboring Mn centres. This was confirmed by control EPR measurements that we performed the in the presence of glycerol where a better resolution, still limited though, of the hyperfine lines is observed (data not shown). The weak couplings in the presence of bicarbonate, do not result in formation of specific dimeric Mn-complexes.

When $(COONH_4)_2{\cdot}H_2O$ was used as additive, a significant change is observed in the EPR spectrum (spectrum (g)). A strong derivative is dominating the EPR spectrum flanked by groups of well-resolved hyperfine splittings, see inset in Fig. 9. These splittings are better resolved in the inset in Fig. 9, have no regular spacing, nei-

ther intensity distribution. This spectrum can be simulated by assuming one Mn^{2+} ($S = 5/2$, $I = 5/2$) using a large D parameter, i.e. $D = 2.6 \pm 0.4$ GHz. We underline that the spectrum in Fig. 9(g) is *not* due to a dinuclear–Mn complex. Such spectra can be easily confused with dinuclear–Mn(II) complexes which, in the strong coupling limit, should be characterized by a ^{55}Mn hyperfine splitting A(^{55}Mn) which is 1/2 of the A(^{55}Mn) of the mononuclear Mn(II) centres [36]. In the complexes studied here, the EPR spectra in Fig. 9, have A(^{55}Mn) in the range 92–108 Gauss therefore a dinuclear–Mn(II) complex should have a A(^{55}Mn) of the order of 46–55 Gauss. The Mn(II) spectra in the presence of oxalate, shown in expanded scale for the sake of the analysis in Fig. 11, have hyperfine splittings A(^{55}Mn) = 75–110 Gauss, see for example the marked splittings in Fig. 11. This clearly shows that this is a *mononuclear* Mn(II) spectrum. Further analysis by computer simulation convincingly attributes it to a mononuclear Mn(II) whose unusually high D value is the origin of the spread-out EPR lineshape with many non-overlapping hyperfine features popping up at a wide range of the resonance field. Thus the EPR data show that most likely oxalate is strongly coordinated at the Mn(II) center.

Therefore the data in Fig. 9 demonstrate that (a) $MnCl_2/L_A$ in 1:1 acetone:MeOH is forming mononcuclear Mn^{2+} complexes with particularly weak ligand field. (b) $(COONH_4)_2{\cdot}H_2O$ alters strongly the ligand field of the Mn^{2+} by direct coordination to the Mn^{2+}. (c) NH_4HCO_3 or $NaHCO_3$ cause a broadening of the Mn EPR spectra, most likely *via* non-specific weak magnetic interactions of neighboring Mn centres. (d) CH_3COONH_4 or $HCOONH_4$ cause only EPR lineshape changes due to small changes in the Zero Field Splitting parameter D.

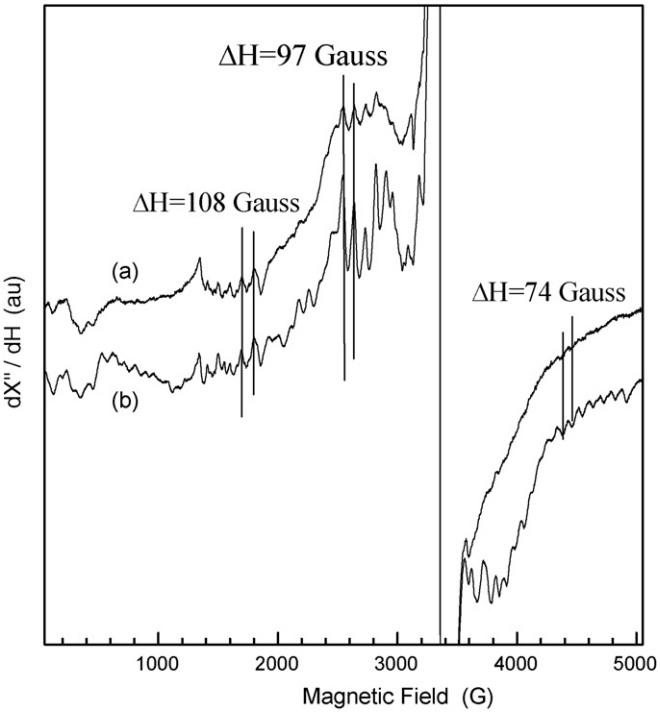

Fig. 11. Expanded view of the EPR spectra for [L_{acac}-Mn + $(COONH_4){\cdot}H_2O$]. (a) Without, (b) with H_2O_2 (350 mV). The spectra are the same shown in Figs. 9 and 10.

3.6.2. *Binary additive [H_2O_2 + salt]*

The EPR spectra in Fig. 10 show the coordination effect of additives on $MnCl_2/L_A$ which was pre-oxidized at 350 mV by 20 μl of H_2O_2. When compared with the addition of CH_3COONH_4 alone, Fig. 9(d), the presence of H_2O_2 plus CH_3COONH_4 caused a significant decrease of the EPR intensity, i.e. by 60–70%, with no further changes in the lineshape, Fig. 10(b). In contrast no intensity change is caused in the presence of H_2O_2 + $HCOONH_4$, compare Figs. 9(d) and 10(c).

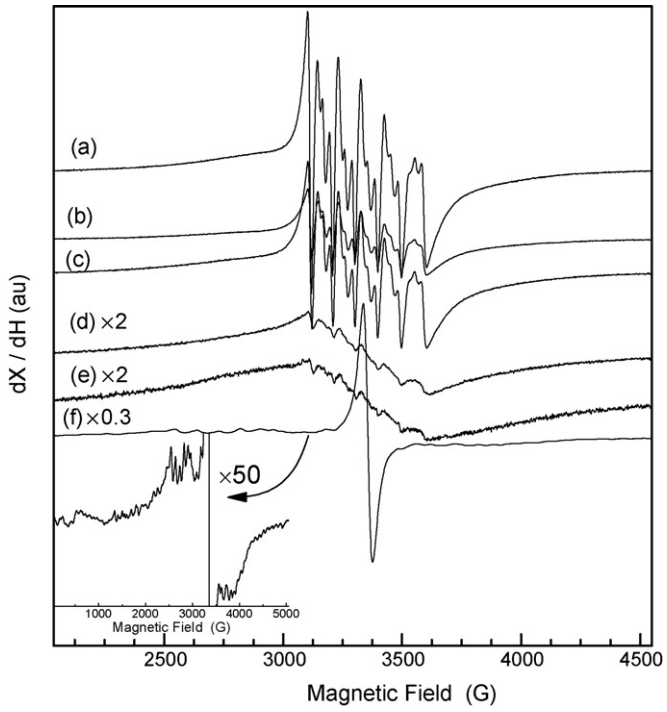

Fig. 10. (a) EPR spectrum of the $MnCl_2/L_A$ pre-oxidized by 20 μl H_2O_2, (b) CH_3COONH_4, (c) $HCOONH_4$, (d) NH_4HCO_3, (e) $NaHCO_3$, (f) $(COONH_4)_2{\cdot}H_2O$. Inset: partial zoom of spectrum (f).

In the presence of H_2O_2 plus bicarbonate salts, i.e. NH_4HCO_3 or $NaHCO_3$ an intensity loss by 50% and 30% is observed, respectively, relative to bicarbonate salts alone, Fig. 9(e) and (f) *vs*. Fig. 10(d) and (e). Finally addition of $(COONH_4)_2{\cdot}H_2O$ after H_2O_2, gives the characteristic EPR lineshape, Fig. 10(g) as in the case of oxalate alone with only small differences in the resolution. The spectra for $(COONH_4)_2{\cdot}H_2O$ are better viewed in Fig. 11 without (a) or with (b) H_2O_2. In both cases the EPR spectra in Fig. 11 are characteristic of a mononuclear Mn^{2+} complex with a large-D value. When compare the intensities of the EPR spectra for Mn(II) in the presence [$(COONH_4)_2{\cdot}H_2O$ plus H_2O_2] *vs*. $(COONH_4)_2{\cdot}H_2O$ alone the data in Fig. 11 shows no significant differences in the EPR intensity.

Overall, the EPR data show that the $MnCl_2/L_A$ complex in 1:1 acetone:MeOH at 350 mV, i.e. in the presence of H_2O_2, plus additive salts, is forming mononcuclear Mn(II) complexes. In the case of H_2O_2 plus CH_3COONH_4 or NH_4HCO_3 a significant decrease of the Mn(II) EPR intensity was observed with no lineshape changes. This decrease can be most easily explained by oxidation of Mn(II) to higher oxidation states, i.e. such as Mn(III) ($S = 2$) or Mn(IV) ($S = 1$), which are not EPR detectable. However, no spectral changes have been observed in Vis-spectra (see Fig. S6 in Supporting information). In this context, the partial EPR signal loss in the presence of bicarbonate salts can be attributed to Mn(II) oxidation, however in a smaller number of Mn-centres than in the case of acetate salts.

Thus the analysis of the EPR data indicates that acetate or bicarbonate salts can promote Mn(II) oxidation. Acetate salts have a decisively more beneficial effect that bicarbonate salts. On the other hand oxalate or formate salt, appear to cause no Mn(II) oxidation, i.e. no EPR intensity change. Oxalate appears to cause only a strong ligand-field alteration (increased D value).

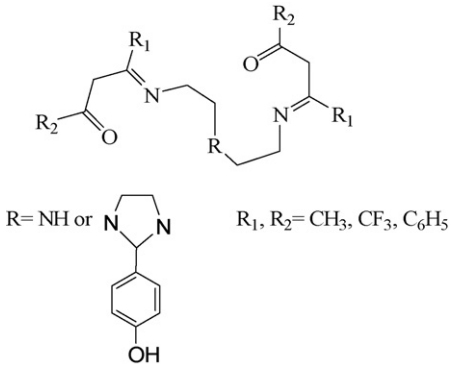

Scheme 2. Molecular structure of acetylacetone-based ligands.

Overall the present EPR data provide two pieces of information. (a) The EPR intensity changes can be explained if we assume that the additives on the Mn(II) cause changes of the redox potential ΔE of the couple Mn(II)/Mn(III) in the order:

$$\Delta E_{(Mn^{2+/3+})}[\text{acetate}] < \Delta E_{(Mn^{2+/3+})}[\text{bicarbonate}] \ll \Delta E_{(Mn^{2+/3+})}[\text{formate}] \sim \Delta E_{(Mn^{2+/3+})}[\text{oxalate}] \sim \Delta E_{(Mn^{2+}/Mn^{3+})}[\text{no salt added}] \quad (1)$$

Though no detailed redox titrations have been performed, the solution potential 350 mV appears to be near a threshold for the Mn(II)/Mn(III) oxidation step. (b) The Zero Field splitting, *D* values, show that Mn(II)/L_A in the presence of acetate or formate has comparable, low, *D*-values. Mn(II)/L_A in the presence of oxalate has a characteristic high *D* value. Bicarbonate results in broad spectra with very weak Mn–Mn interactions and most likely no severe *D* value changes.

3.7. Mechanistic aspects

3.7.1. Structural aspects

Recently, various acetylacetone-based ligands have been designed and synthesized in our lab in order to form dinuclear metal complexes as potential epoxidation catalysts [31]. The general structure of these ligands is depicted in Scheme 2, where R represents the connecting spacer and R_1, R_2 are alkyl or aryl substituents, respectively. The ligands presented here bear an imidazolidine derivative marked R in Scheme 2, and CH_3 and CF_3 groups marked R_1 and R_2, respectively.

The ligands are potentially heptadentate, with the long flexible chelating arms able to bridge up to two-Mn ions. However, the EPR data clearly show that in MnL_A complexes in solution, no magnetic interaction between Mn(II) centers is detected. The same result was reported recently [31] based on EPR spectroscopy for Mn(II) complexes with other ligands of the same family, i.e. acetylacetone-based Schiff bases. Of importance, is that all these ligands when complexed with Mn(II) show good catalytic activity. This demonstrates clearly that mononuclear manganese complexes, as those described here, can be efficient catalysts.

Literature reports show that simple carboxylates bridge efficiently neighbouring Mn(II) centres, which is easily detected by EPR spectroscopy [33]. However, the present EPR data for the MnL_A complexes show that acetate does not result in Mn-dimers. In addition, the catalytic results show no difference for acetate-based-catalysts *vs*. chloride-based-catalysts.

When we inspect the influence of the nature of the connecting bridge R and the R_1, R_2 substituents on the catalytic properties, we notice that the catalytic systems based on either these ligands are equally efficient. Moreover only small changes were observed on the catalytic activity by modifying the R, R_1 and R_2 substituents, while in all the tested structures, the first coordination sphere of the Mn center was unaltered. All together this information indicates that the oxygen transfer ability of the mononuclear active intermediate mainly depends on the first coordination sphere of the manganese center. Side chain modifications play no- or a secondary role in the catalytic activity.

3.7.2. Role of additives

At face value, the observed catalytic improvement induced by CH_3COONH_4, can be attributed to two possible reasons. One is the possibility that CH_3COONH_4 could be act as a coordinative agent. A second possibility is the formation of dimeric Mn-complexes. However, according to EPR data, only mononuclear Mn(II) complexes are formed. Moreover, the presence of CH_3COONH_4 has a resolvable small influence on the *D* parameter, which strongly disfavours a CH_3COONH_4 having strong ligand field effect on the Mn. A similar conclusion can be reached for formate, i.e. $HCOONH_4$. These results show that the role of CH_3COONH_4 does not involve a severe structural modification of the first coordination sphere on Mn(II).

In contrast, a strong structural modification is evidenced by EPR spectroscopy when the oxalate adduct $(COONH_4)_2{\cdot}H_2O$ was used as additive, i.e. a large *D* value. The straightforward explanation is that oxalate is directly coordinated at the Mn(II) and this strong structural modification is accompanied with very poor catalytic results.

The effect of NH_4HCO_3 appears to be different. It causes a severe broadening of the EPR spectra, while a partially resolved hyperfine pattern remains resembling the spectrum of Mn(II)/L_A. The line broadening most likely indicates that in the majority of the centres, neighboring Mn-centres interact non-specifically, e.g. *via* weak couplings. The partially resolved hyperfine pattern shows that in a fraction of the centres the *D* parameter remains unaltered. A more specific interpretation of the NH_4HCO_3 EPR data could not be attempted with the data at hand. However, we consider that NH_4HCO_3 is rather weakly coupled with the Mn(II) centres, in a manner intermediate between acetate and oxalate. The catalytic results for NH_4HCO_3 are intermediate of those between acetate (high yield) and oxalate (low yield). Interestingly this ranking bears relevance to the changes in redox potential as described in expression (1).

Overall, the present analysis provides useful information which highlight the, not obvious to explain, effects of additives on structure/catalytic properties of MnL_A. (a) Additives that allow easier oxidation of Mn(II) to higher oxidation states, i.e. such as acetate and bicarbonate, can promote decisively the catalytic function. (b) Additives that do not allow oxidation of Mn(II) to higher oxidation states, i.e. such as formate and oxalate, inhibit severely the catalytic function. (c) Monocarboxylate ions, i.e. acetate, bicarbonate and formate do not disturb considerably the first coordination sphere of Mn(II). (d) Dicarboxylate additives, i.e. such as oxalate, form strong complex with the Mn(II).

At this point it is of pertinence to highlight the beneficial role of NH_4^+ as counter-cation of the additives in the catalytic procedure. By using CH_3COONa instead of CH_3COONH_4 no-epoxidation yields are obtained. Based on this, in conjunction with the fact that the optimal product yield was obtained when the ratio [substrate:CH_3COONH_4] was ~[1:1], we propose that CH_3COONH_4 probably acts as a dual acid-base system participating into the catalytic cycle. This can be either as a proton-donor or as a proton-acceptor. In this context, the relatively good catalytic results obtained by NH_4HCO_3 can be also be attributed to the presence of NH_4^+.

3.8. Conclusions

Two new symmetrical acetylacetone-based Schiff bases L_A, L_B have been synthesized. Their complexes with Mn(II) have been evaluated as homogeneous catalytic systems for alkene epoxidation with H_2O_2. The results presented here demonstrate their remarkable effectiveness and selectivity but only in the presence of additives such as ammonium acetate.

The enhanced reactivity of the present ligands with Mn(II) as epoxidation catalysts is not modified by groups which are not involved in the first metal coordination sphere.

We suggest that the determinant role of the additive is (a) to promote Mn^{2+} oxidation by lowering the redox potential ΔE of the couple Mn(II)/Mn(III) and (b) to act as a dual acid-base system. Additives that allow easier oxidation of Mn(II) to higher oxidation states, i.e. such as acetate and bicarbonate, can promote decisively the catalytic function. Additives that do not allow oxidation of Mn(II) to higher oxidation states, i.e. such as formate and oxalate, inhibit severely the catalytic function.

EPR spectroscopy shows that the catalytic centre is a mononuclear Mn complex. Monocarboxylate ions, i.e. acetate, bicarbonate and formate do not disturb considerably the first coordination sphere of Mn(II). Dicarboxylate additives, i.e. such as oxalate, form strong complex with the Mn(II).

Acknowledgements

The authors thank the postgraduate program “Bioinorganic Chemistry” at the Department of Chemistry at the University of Ioannina and Dr. A. Badeka for mass spectra obtained on a machine funded by the Network of Horizontal Laboratory and Unit Centres of the University of Ioannina.

Appendix A. Supplementary data

Supplementary data associated with this article can be found, in the online version, at doi:10.1016/j.molcata.2008.09.019.

References

[1] E.J. Larson, V.L. Pecoraro, in: V.L. Pecoraro (Ed.), Manganese Redox Enzymes, VCH, New York, 1992.
[2] B. Meunier, Biomimetic Oxidations Catalyzed by Transition Metal Complexes, Imperial College Press, London, 2000.
[3] S. Tanase, E. Bouwman, Adv. Inorg. Chem. 58 (2006) 29.
[4] P. Pietikainen, Tetrahedron 54 (1998) 4319.
[5] R. Irie, K. Noda, Y. Ito, N. Matsumoto, T. Katsuki, Tetrahedron Lett. 31 (1990) 7345.
[6] W. Zhang, J.L. Loebach, S.R. Wilson, E.N. Jacobsen, J. Am. Chem. Soc. 112 (1990) 2801.
[7] R. Irie, N. Hosoya, T. Katsuki, Synlett (1994) 255.
[8] L. Cavallo, H. Jacobsen, Eur. J. Inorg. Chem. (2003) 892.
[9] B. Meunier, Chem. Rev. 92 (1992) 1411.
[10] G.B. Shul'pin, J. Mol. Catal. A: Chem. 189 (2002) 39.
[11] P. Pietikainen, J. Mol. Catal. A: Chem. 165 (2001) 73.
[12] T. Schwenkreis, A. Berkessel, Tetrahedron Lett. 34 (1993) 4785.
[13] P. Pietikainen, Tetrahedron Lett. 35 (1994) 941.
[14] M. Hoogenraad, K. Ramkisoensing, H. Kooijman, A.L. Spek, E. Bouwman, J.G. Haasnoot, J. Reedijk, Inorg. Chim. Acta 279 (1998) 217.
[15] M. Hoogenraad, K. Ramkisoensing, W.L. Driessen, H. Kooijman, A.L. Spek, E. Bouwman, J.G. Haasnoot, J. Reedijk, Inorg. Chim. Acta 320 (2001) 117.
[16] R. Hage, J.E. Iburg, J. Kerschner, J.H. Keek, E.L.M. Lempers, R.J. Martens, U.S. Racherla, S.W. Russel, T. Swarthoff, M.R.P. van Vliet, J.B. Warnaar, L. Van der Wolf, B. Krijnen, Nature 369 (1994) 637.
[17] D. De Vos, T. Bein, Chem. Commun. (1996) 917.
[18] V.C. Quee Smith, L. DelPizzo, S.H. Jureller, J.L. Kerschner, R. Hage, Inorg. Chem. 35 (1996) 6461.
[19] D.E. De Vos, B.F. Sels, M. Reynaers, Y.V.S. Rao, P.A. Jacobs, Tetrahedron Lett. 39 (1998) 3221.
[20] A. Berkessel, C.A. Sklorz, Tetrahedron Lett. 40 (1999) 7965.
[21] J. Brinksma, L. Schmieder, G. Van Vliet, R. Boaron, R. Hage, D.E. De Vos, P.L. Alsters, B.L. Feringa, Tetrahedron Lett. 43 (2002) 2619.
[22] C.B. Woitiski, Y.N. Kozlov, D. Mandelli, G.V. Nizova, U. Schuchardt, G.B. Shul'pin, J. Mol. Catal. A: Chem. 222 (2004) 103.
[23] J.W. de Boer, J. Brinksma, W.R. Browne, A. Meetsma, P.L. Alsters, R. Hage, B.L. Feringa, J. Am. Chem. Soc. 127 (2005) 7990.
[24] J.W. de Boer, W.R. Browne, J. Brinksma, P.L. Alsters, R. Hage, B.L. Feringa, Inorg. Chem. 46 (2007) 6353.
[25] B.S. Lane, K. Burgess, J. Am. Chem. Soc. 123 (2001) 2933.
[26] B.S. Lane, M. Vogt, V.J. DeRose, K. Burgess, J. Am. Chem. Soc. 124 (2002) 11946.
[27] J. Brinksma, R. Hage, J. Kerschner, B.L. Feringa, Chem. Commun. (2000) 537.
[28] D. Zois, Ch. Vartzouma, Y. Deligiannakis, N. Hadjiliadis, L. Casella, E. Monzani, M. Louloudi, J. Mol. Catal. A 261 (2007) 306.
[29] A. Serafimidou, A. Stamatis, M. Louloudi, Catal. Commun. 9 (2008) 35.
[30] M. Louloudi, Ch. Kolokytha, N. Hadjiliadis, J. Mol. Catal. A 180 (2002) 19.
[31] Ch. Vartzouma, E. Evaggellou, Y. Sanakis, N. Hadjiliadis, M. Louloudi, J. Mol. Catal. A 263 (2007) 77.
[32] U. Mukhopadhyay, L.R. Falvello, D. Ray, Eur. J. Inorg. Chem. (2001) 2823.
[33] G.H. Reed, G.D. Markham, in: L.J. Berliner, J. Reuben (Eds.), Biological Magnetic Resonance, vol. 6, Plenum, New York, 1984, pp. 73–142.
[34] S. Misra, Physica B 203 (1994) 193.
[35] B.T. Allen, J. Chem. Phys. 43 (1965) 3820.
[36] A. Bencini, D. Gatteschi, Electron Paramagnetic Resonance of Exchange Coupled Systems, Springer–Verlag, Berlin, 1990.